

Weyl Superfluidity in a Three-dimensional Dipolar Fermi Gas

Bo Liu,^{1,2,*} Xiaopeng Li,³ Lan Yin,⁴ and W. Vincent Liu^{1,2,†}

¹*Wilczek Quantum Center, Zhejiang University of Technology, Hangzhou 310023, China*

²*Department of Physics and Astronomy, University of Pittsburgh, Pittsburgh, PA 15260, USA*

³*Condensed Matter Theory Center and Joint Quantum Institute,
University of Maryland, College Park, MD 20742, USA*

⁴*School of Physics, Peking University, Beijing 100871, China*

Weyl superconductivity or superfluidity, a fascinating topological state of matter, features novel phenomena such as emergent Weyl fermionic excitations and anomalies. Here we report that an anisotropic Weyl superfluid state can arise as a low temperature stable phase in a 3D dipolar Fermi gas. A crucial ingredient of our model is a direction-dependent two-body effective attraction generated by a rotating external field. Experimental signatures are predicted for cold gases in radio-frequency spectroscopy. The finite temperature phase diagram of this system is studied and the transition temperature of the Weyl superfluidity is found to be within the experimental scope for atomic dipolar Fermi gases.

Weyl superfluids or semimetals represent recent developments in generalizing topological phases from gapped to gapless systems (e.g., from topological insulators to semimetals), in condensed matter physics [1, 2]. These Weyl states are characterized by the presence of two (or more) gapless Weyl points, which are topologically protected against small perturbations. The Weyl nodes lead to a variety of fascinating phenomena such as unusual surface states [3, 4], Hall effects [5, 6], and other transport features [7, 8]. Finding electronic materials supporting Weyl states has attracted considerable interests [9]. There are many proposed potential candidate materials, such as the pyrochlore iridates [3], topological insulator multilayer structures [7, 10–12], as well as certain quasicrystals [13]. However, there is still no compelling experimental evidence for the observation of one. In the field of ultracold atoms, this phase was predicted to appear in spin-orbit coupled Fermi gases [14, 15]. This line of active research awaits for the future experimental breakthrough of synthesizing higher dimensional artificial spin-orbit coupling with controlled heating [16]. After all, the search for Weyl superconductors remains an open problem for both electronic and ultracold atomic systems.

In this letter, we report the emergence of Weyl superfluidity in a 3D single-component dipolar Fermi gas with an effective attraction engineered by a rotating external field. Recently, degenerate dipolar Fermi gases witnessed rapid developments in both magnetic dipolar atoms (such as ¹⁶⁷Er [17, 18] and ¹⁶¹Dy [19, 20] atoms) and polar molecules [21, 22], stimulating tremendous interests in dipolar effects in many-body phases. The effects of the anisotropic dipolar interaction on the fermion many-body physics have been extensively investigated [23]. In particular, this provides the possibility of superfluid pairing between dipolar Fermi atoms in spinless or multicomponent systems [24–27] at low temperatures. For dipoles aligned parallel to the z direction, a p -wave superfluid state with the dominant p_z symmetry was studied in a three-dimensional dipolar Fermi gas [28] and the competition between this superfluidity and nematic charge-density-wave (CDW) was also discussed [29]. For a dipolar Fermi gas confined in a 2D plane, superfluid states of p -wave symme-

try [30–32], including a $p + ip$ state in particular [31, 32], are predicted.

The key idea here is to engineer a direction-dependent two-body effective attraction, which supports Cooper pairs with the chirality encoded in the p -wave pairing gap. This Weyl superfluid state breaks time reversal symmetry as well as inversion symmetry. Such broken symmetries have profound implications for the interesting topological defects [1]. We shall describe this state in a 3D magnetic dipolar Fermi gas composed of one hyperfine state, which has been realized in the experimental system of ¹⁶⁷Er [17] recently. The direction of dipole moments can be fixed by applying an external magnetic field. Let the external field be orientated at a small angle with respect to the xy -plane and rotate fast around the z axis. The time-averaged interaction between dipoles [33] is isotropically attractive in the xy -plane and repulsive in the z -direction. In general, the attraction is expected to cause Cooper pairing instability while the repulsion should restrict the pairing from certain nodal directions. Their combined effect could give rise to Weyl Fermi points for the Bogoliubov quasi-particles. Such a heuristically argued result is indeed confirmed by a self-consistent calculation through the model to be introduced below.

Effective model. Consider a 3D spinless dipolar Fermi gas subjected to an external rotating magnetic field

$$\mathbf{B}(t) = B[\hat{z} \cos \varphi + \sin \varphi(\hat{x} \cos \Omega t + \hat{y} \sin \Omega t)],$$

where Ω is the rotation frequency, B is the magnitude of magnetic field, the rotation axis is z , and φ is the angle between the magnetic field and the z axis. In strong magnetic fields, dipoles are aligned parallel to $\mathbf{B}(t)$. With fast rotations, the effective interaction between dipoles is the time-averaged interaction

$$V(\mathbf{r}) = \frac{d^2(3\cos^2\varphi-1)}{2r^3}(1-3\cos^2\theta) \equiv \frac{d'^2}{r^3}(1-3\cos^2\theta),$$

where $d'^2 \equiv d^2 \frac{3\cos^2\varphi-1}{2}$ with the magnetic dipole moment d , \mathbf{r} is the vector connecting two dipolar particles, and θ is the angle between \mathbf{r} and the z axis. The effective attraction,

$V(\mathbf{r}) < 0$, is created by making $\cos \varphi < \sqrt{1/3}$, which is our focus in this work.

The effective Hamiltonian of the system above is given by $H = \int d^3\mathbf{r} \psi^\dagger(\mathbf{r}) \left[-\frac{\hbar^2 \nabla^2}{2m} - \mu \right] \psi(\mathbf{r}) + \frac{1}{2} \int d^3\mathbf{r} \int d^3\mathbf{r}' \psi^\dagger(\mathbf{r}) \psi^\dagger(\mathbf{r}') V(\mathbf{r} - \mathbf{r}') \psi(\mathbf{r}') \psi(\mathbf{r})$, where $\psi(\mathbf{r})$ is the fermion field and μ is the chemical potential.

Due to the attractive interaction, fermions tend to pair with each other and form a superfluid state at low temperatures. To study this superfluid state, we construct a general theory to describe a spinless Fermi gas by a fully self-consistent Hartree-Fock-Bogoliubov method. The details are given in Supplementary Materials. Constructing a bosonic effective action by Hubbard-Stratonovich transformation, we obtain self-consistent equations under a saddle-point approximation for the fermion bilinears $\kappa(\mathbf{r}) = \int d^3\mathbf{r}' V(\mathbf{r} - \mathbf{r}') \psi^\dagger(\mathbf{r}') \psi(\mathbf{r})$, $\lambda(\mathbf{r}, \mathbf{r}') = -V(\mathbf{r} - \mathbf{r}') \psi^\dagger(\mathbf{r}) \psi(\mathbf{r}')$, and $\tilde{\Delta}(\mathbf{r}, \mathbf{r}') = V(\mathbf{r} - \mathbf{r}') \psi(\mathbf{r}') \psi(\mathbf{r})$. Correspondingly, the Hartree-Fock self-energy and superconducting gap are given as

$$\begin{aligned} \Sigma(\mathbf{r}', \mathbf{r}) &\equiv \langle \kappa(\mathbf{r}) \rangle \delta(\mathbf{r} - \mathbf{r}') + \langle \lambda(\mathbf{r}', \mathbf{r}) \rangle, \\ \Delta(\mathbf{r}', \mathbf{r}) &\equiv \langle \tilde{\Delta}(\mathbf{r}', \mathbf{r}) \rangle, \end{aligned} \quad (1)$$

where $\langle \dots \rangle$ means the expectation value in the ground state.

3D uniform dipolar Fermi gas. We now apply the general theory outlined above to the system of a 3D uniform spinless dipolar Fermi gas in the presence of a rotating magnetic field. From the symmetry of the system, at least for not too strong interaction strength, we anticipate that pairing only occurs between a particle with momentum \mathbf{k} and another with momentum $-\mathbf{k}$ as in the standard BCS theory. Due to the translational symmetry, it is convenient to study this problem in the momentum space. After Fourier transformation of Eq. (1), the Hartree-Fock self-energy and the pairing gap read

$$\Sigma_{\mathbf{k}} = V(0)n - \frac{1}{v} \sum_{\mathbf{k}'} V(\mathbf{k} - \mathbf{k}') \frac{1}{2} \left[1 - \frac{\xi_{\mathbf{k}'}}{E_{\mathbf{k}'}} \tanh\left(\frac{\beta}{2} E_{\mathbf{k}'}\right) \right], \quad (2)$$

$$\Delta_{\mathbf{k}} = -\frac{1}{v} \sum_{\mathbf{k}'} V(\mathbf{k} - \mathbf{k}') \frac{\Delta_{\mathbf{k}'}}{2E_{\mathbf{k}'}} \tanh\left(\frac{\beta}{2} E_{\mathbf{k}'}\right), \quad (3)$$

where $E_{\mathbf{k}}$ is the quasi-particle excitation energy given by $E_{\mathbf{k}} = \sqrt{\xi_{\mathbf{k}}^2 + |\Delta_{\mathbf{k}}|^2}$ with the kinetic energy of fermions $\xi_{\mathbf{k}} = \varepsilon_{\mathbf{k}} + \Sigma_{\mathbf{k}} - \mu$ and $\varepsilon_{\mathbf{k}} = \frac{\hbar^2 k^2}{2m}$. The interaction between two dipoles in the momentum space is given by $V(\mathbf{q}) = \frac{4\pi d^2}{3} (3 \cos^2 \theta_{\mathbf{q}} - 1)$, with the angle $\theta_{\mathbf{q}}$ between momentum \mathbf{q} and z axis, n is the total density, v is the volume, and $\beta = 1/(k_B T)$.

It is known that the gap equation (Eq. (3)) has ultraviolet divergence [26]. The origin of the divergence can be attributed to the singularity of the dipolar interaction potential for large momentum, or equivalently for short distance. Just as in the treatment of two-component Fermi gas with contact interaction [34], we need to regularize the interaction in the gap equation (Eq. (3)). The divergence can be eliminated by expressing the bare interaction $V(\mathbf{k} - \mathbf{k}')$ in Eq. (3) in terms of the vertex function (scattering off-shell amplitude) [35] as

$\Gamma(\mathbf{k} - \mathbf{k}') = V(\mathbf{k} - \mathbf{k}') - \frac{1}{v} \sum_{\mathbf{q}} \Gamma(\mathbf{k} - \mathbf{q}) \frac{1}{2\varepsilon_{\mathbf{q}}} V(\mathbf{q} - \mathbf{k}')$, and the gap equation will be renormalized as

$$\Delta(\mathbf{k}) = -\frac{1}{v} \sum_{\mathbf{k}'} \Gamma(\mathbf{k} - \mathbf{k}') \Delta(\mathbf{k}') \left[\frac{\tanh\left(\frac{\beta E_{\mathbf{k}'}}{2}\right)}{2E_{\mathbf{k}'}} - \frac{1}{2\varepsilon_{\mathbf{k}'}} \right]. \quad (4)$$

Note that the Hartree term for the selfenergy in Eq. (2), $V(0)n$ vanishes, since for dipolar interaction in 3D uniform system, $V(0) = 0$ [36] and renormalization of the interaction has a negligible effect on the self-energy. Then, the Hartree-Fock self-energy is expressed as

$$\Sigma_{\mathbf{k}} = -\frac{1}{v} \sum_{\mathbf{k}'} V(\mathbf{k} - \mathbf{k}') \frac{1}{2} \left[1 - \frac{\xi_{\mathbf{k}'}}{E_{\mathbf{k}'}} \tanh\left(\frac{\beta}{2} E_{\mathbf{k}'}\right) \right]. \quad (5)$$

The total density n can be obtained from the thermodynamic potential Ω by using the relation $N = -\partial\Omega/\partial\mu$,

$$n = \sum_{\mathbf{k}} \frac{1}{2v} \left[1 - \frac{\xi_{\mathbf{k}}}{E_{\mathbf{k}}} \tanh\left(\frac{\beta}{2} E_{\mathbf{k}}\right) \right]. \quad (6)$$

Under the constraint of Fermi statistics for this single component dipolar Fermi gas, the dominant pairing instability is in the channel with orbital angular momentum $L = 1$. The most stable low temperature phase has $p_x + ip_y$ symmetry, following from the fact that this phase fully gaps the Fermi surface, in contrast to competing phases, such as p_x or p_y superfluid state [37]. Note that in the presence of a rotating magnetic field, all the dipoles rotating with respect to the z -axis, so the system has a $SO(2)$ spatial rotation symmetry. This symmetry is not broken in the $p_x + ip_y$ pairing state, and we can thus write down the Cooper pair as $\Delta_{\mathbf{k}} \equiv \Delta(k_\rho, k_z) e^{i\varphi_{\mathbf{k}}}$, where $k_\rho = \sqrt{k_x^2 + k_y^2}$ and $\varphi_{\mathbf{k}}$ is the polar angle of the momentum \mathbf{k} in the xy -plane, to simplify the calculation in Hartree-Fock-Bogoliubov approach.

Weyl fermions. With the time-reversal symmetry spontaneously broken in the superfluid state, topological properties emerge in quasi-particle excitations, which are described by a mean field Hamiltonian $H_{SF} = \sum_{\mathbf{k}} [\xi_{\mathbf{k}} c_{\mathbf{k}}^\dagger c_{\mathbf{k}} + \frac{\Delta_{\mathbf{k}}^*}{2} c_{-\mathbf{k}} c_{\mathbf{k}} + \frac{\Delta_{\mathbf{k}}}{2} c_{\mathbf{k}}^\dagger c_{-\mathbf{k}}^\dagger]$, with $c_{\mathbf{k}}$ the fermion annihilation operator. This Hamiltonian can be expressed in the matrix form by

$$\begin{aligned} H_{SF} &= \sum_{\mathbf{k}} (c_{\mathbf{k}}^\dagger, c_{-\mathbf{k}}) \begin{pmatrix} \frac{\xi(\mathbf{k})}{2} & \frac{\Delta(\mathbf{k})}{2} \\ \frac{\Delta^*(\mathbf{k})}{2} & -\frac{\xi(\mathbf{k})}{2} \end{pmatrix} \begin{pmatrix} c_{\mathbf{k}} \\ c_{-\mathbf{k}}^\dagger \end{pmatrix} \\ &\equiv \sum_{\mathbf{k}} (c_{\mathbf{k}}^\dagger, c_{-\mathbf{k}}) \vec{d}(\mathbf{k}) \cdot \vec{\sigma} \begin{pmatrix} c_{\mathbf{k}} \\ c_{-\mathbf{k}}^\dagger \end{pmatrix}. \end{aligned}$$

where the \vec{d} vector is defined in terms of the Pauli matrices $\vec{\sigma}$'s. The $d_{x,y}$ components vanish along the k_z axis, whereas along this axis, d_z vanishes at only two points $\mathbf{k}_+^C = (0, 0, k_+^C)$ and $\mathbf{k}_-^C = (0, 0, k_-^C) (= -\mathbf{k}_+^C)$ (Fig. 1a). In the (k_x, k_y) momentum plane with $k_-^C < k_z < k_+^C$, $\vec{d}(\mathbf{k})$ wraps around a sphere as shown in Fig. 1b. Evidently, it points to the south pole on the k_z axis, while with increasing k_ρ , the $\vec{d}(\mathbf{k})$ vector varies continuously and eventually points to the north pole as $k_\rho \rightarrow \infty$. This vector $\vec{d}(\mathbf{k})$ thus forms a skyrmion in the momentum space with a topological charge ± 1 (where the ‘ \pm ’

sign reveals the spontaneous time-reversal symmetry breaking). However, in other regions $k_z > k_+^C$ or $k_z < k_-^C$, the topological charge vanishes. These two gapless points \mathbf{k}_\pm^C are Weyl nodes, defining the corresponding topological transitions in the momentum space [7, 15]. Close to the Weyl nodes, the Hamiltonian takes the form of 2×2 Hamiltonian of a chiral Weyl fermion [38]. We have checked that the quasi-particle energy dispersion $E_{\mathbf{k}}$ is linear around both two Weyl points, for instance as shown in Fig. 2b when the interaction strength $J = 3$ where $J \equiv |\frac{m d^2}{\hbar^2} k_F|$. As shown in Fig 2c and d, the Weyl nodes are hedgehog-like topological defects of the vector field $\vec{d}(\mathbf{k})$, which are the point source of Berry flux in momentum space, with a topological invariant $N_C = \pm 1$. Here N_C is defined by $N_C = \frac{1}{24\pi^2} \epsilon_{\mu\nu\gamma\chi} \text{tr} \int_{\Sigma} d\mathbb{S}^\chi G \frac{\partial G^{-1}}{\partial k_\mu} G \frac{\partial G^{-1}}{\partial k_\nu} G \frac{\partial G^{-1}}{\partial k_\gamma}$, where G^{-1} is the inverse Green's function for the quasi-particle excitation, Σ is a 3D surface around the isolated Fermi point \mathbf{k}_+^C or \mathbf{k}_-^C , and tr stands for the trace over the relevant particle-hole degrees of freedom [1]. The quasi-particle excitations near the Fermi points realize the long-sought low-temperature analog of Weyl fermions as originally proposed in particle physics. These Weyl nodes are separated from each other in momentum space. They can not be hybridized, which makes them indestructible, as they can only disappear by mutual annihilation of pairs with opposite topological charges. This is the mechanism of topological stability of this Weyl superfluid state, which is distinct from the spectral-gap protection in insulating topological phases. To characterize the existence of Weyl fermions, we calculate the fermionic density of states (DOS) for superconducting states [39, 40] $N(E) = \frac{1}{(2\pi)^3} \int d^3\mathbf{k} \frac{1}{2} (1 + \frac{\xi(\mathbf{k})}{E(\mathbf{k})}) \delta(E - E(\mathbf{k}))$, which is directly related to the radio frequency (rf) spectroscopy signal [41]. With linear dispersion near Weyl nodes, we find $N(E) \propto E^2$ when $E \rightarrow 0$, which is a direct manifestation of Weyl fermions. This behavior of DOS is confirmed in our numerics (Fig. 2a). The experimental advances in rf measurement [42, 43] makes the detection of this signal experimentally accessible.

The other important feature of Weyl fermions realized in this dipolar gas is that they have anisotropic dispersion, reflecting the anisotropy of dipolar interactions. In Fig. 2b, the conic quasi-particle dispersion as a function of the momentum $\mathbf{k} - \mathbf{k}_\pm^C$ is shown. This momentum is chosen with a certain angle θ respecting to the k_z axis. The cones with positive and negative branches correspond to the Bogoliubov quasi-particle energy $\pm E(\mathbf{k} - \mathbf{k}_\pm^C)$. The Fermi velocity, shown by the slope of the quasi-particle dispersion, strongly depends on the angle θ .

Anisotropic superconducting gap. We now discuss the superconducting gap for fermions resulting from anisotropic dipole-dipole interaction. For clarity of demonstration, we take the first-order Born approximation by replacing the vertex function $\Gamma(\mathbf{k} - \mathbf{k}')$ in the gap equation (Eq. (4)) by the bare dipolar interaction $V(\mathbf{k} - \mathbf{k}')$. By numerically solving the Hartree-Fock self-energy equation (Eq. (5)), the gap equation (Eq. (4)), and number equation (Eq. (6)) self-consistently,

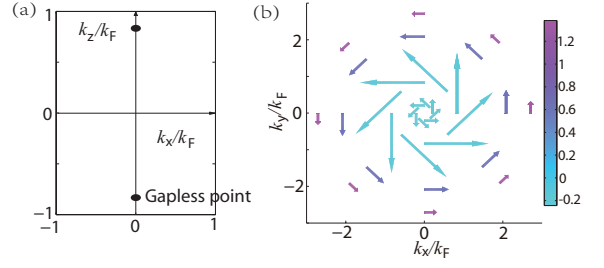


FIG. 1: (a) Gapless points along the k_z axis, where the unit of momentum is the Fermi momentum k_F . (b) Illustration of the skyrmion configuration formed by $\vec{d}(\mathbf{k})$ vector in the (k_x, k_y) plane, with fixed $k_z \in (k_-^C, k_+^C)$. The arrows show $d_{x,y}$ components, and the colors index the d_z component.

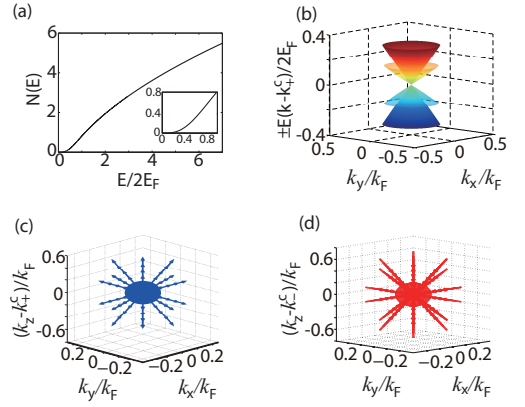


FIG. 2: (a) Density of states (DOS) which has been defined in the main text in units of n_F/E_F , where $n_F = \frac{k_F^3}{6\pi^2}$ and $E_F = \frac{\hbar^2 k_F^2}{2m}$. (b) Quasi-particle dispersion around the gapless points. There are four branches of conic energy spectra shown here. For the two branches in the middle we choose $\theta = \pi/10$, while for the other two we choose $\pi/2$. (c) and (d) Hedgehog-like topological defects formed by the $\vec{d}(\mathbf{k})$ vector around two Weyl nodes.

the superconducting gap anisotropy has been investigated. As shown in Fig. 3a, the magnitude of the order parameter (superconducting gap) on the Fermi surface $\Delta_F(\theta_{\mathbf{k}})$ monotonically increases when enlarging the angle $\theta_{\mathbf{k}}$ between the momentum \mathbf{k} and z axis. The maximum value of $\Delta_F(\theta_{\mathbf{k}})$ is reached in the direction perpendicular to the dipoles, say $\theta_{\mathbf{k}} = \frac{\pi}{2}$. This is because the dipolar interaction is mostly attractive when $\theta_{\mathbf{k}} = \frac{\pi}{2}$. In the direction of the dipoles, namely $\theta_{\mathbf{k}} = 0$ the order parameter vanishes. Fig. 3b shows that the order parameter is also dependent on k_ρ with fixed k_z . This can be understood from the analysis of the gap equation (Eq. (4)) that the main contribution to the integral comes from the region of small momentum which is close to the Fermi surface. In the weak interaction regime, the pairing order parameter is exponentially small, for instance when $J = 3$ it is around $10^{-3} E_F$. However, when the interaction strength increases, the superconducting gap will be comparable to E_F . For ex-

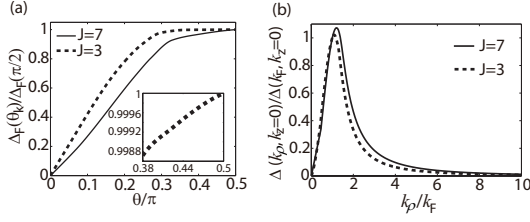


FIG. 3: Anisotropic superconducting pairing order parameter with different interaction strengths $J = 3$ and 7 ($J \equiv |\frac{md^2}{\hbar^2}k_F|$). (a) The superconducting gap $\Delta_F(\theta_{\mathbf{k}})$ on the Fermi surface versus the angle $\theta_{\mathbf{k}}$ between the momentum \mathbf{k} and z axis. (b) The superconducting gap $\Delta(k_{\rho}, k_z)$ as a function of k_{ρ} with fixed k_z .

ample when $J = 15$ it reaches around $0.4E_F$. The anisotropy of the order parameter provides a crucial difference from both s [34] and p -wave pairing [44] due to a short-range attractive interaction. This anisotropy ensures the anisotropic momentum dependence of the gap in the spectrum of single particle excitations. For example, excitations with momenta perpendicular to the direction of the dipoles acquire the largest gap. In contrast to this, the excitations with momenta in the direction of the dipoles remain unchanged. Therefore, the response of this dipolar superfluid Fermi gas to small external perturbations will have a pronounced anisotropic character.

Finite temperature phase transition. Upon increasing temperature the Weyl superfluid state will undergo a phase transition to a normal state. By numerically solving the Hartree-Fock self-energy equation (Eq. (5)), gap equation (Eq. (4)), and number equation (Eq. (6)) self-consistently at finite temperature, the BCS transition temperature is obtained as shown in Fig. 5. We find that the BCS transition temperature is a monotonically increasing function of the interaction strength J . However, the strong enough interaction will cause the system to suffer from the mechanical instability. The reason for that is as follows. The magnitude of superconducting gap increases with enhancing the interaction strength. Due to the attractive nature of the effective interaction between dipoles, the free energy of this dipolar gas is smaller than that of an ideal Fermi gas. This energy reduction increases with the interaction strength (or equivalently the density of the gas with a certain dipole moment). When the interaction strength is large enough, the effect of the interaction is dominant and the system can be unstable. As shown in Fig. 4, the chemical potential is a monotonically decreasing function when the density is above a critical value, and the compressibility is negative, indicating that the superfluid state is dynamically unstable. By considering the mechanical instability of the system, as shown in Fig. 5, the finite temperature phase diagram is obtained. We find that the BCS transition temperature of a stable superfluid state can reach around $0.2E_F$ at mean-field level, which approaches to the current experimental temperature region [17, 19].

In the current experiments, for example, ^{167}Er atom's magnetic dipole moment is $7\mu_B$ and the density of the system

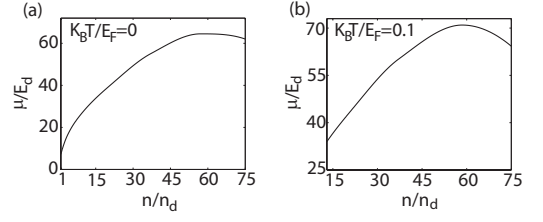


FIG. 4: Chemical potential μ versus the density n . In (a), the temperature is $T = 0$, while in (b) the temperature is $k_B T = 0.1E_F$. Here, the unit of μ is $E_d \equiv \hbar^6/(m^3 d^4)$ and the unit of n is $n_d \equiv [\hbar^2/(md^2)]^3$.

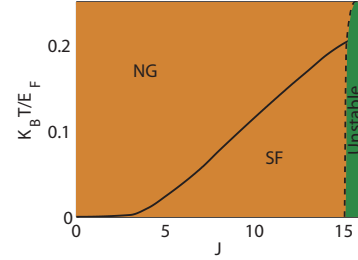


FIG. 5: Finite temperature phase diagram—The solid line stands for the BCS transition temperature which separates the region between the superfluid state (SF) and normal state (NG). The area on the right hand side of the dash line demonstrates the instability of the system due to the strongly attractive interaction.

is about $n = 4 \times 10^{14} \text{cm}^{-3}$. The Fermi energy is given by $E_F = \frac{\hbar^2}{2m}(6\pi^2 n)^{2/3} \approx 0.16 \text{MHz}$ and the corresponding Fermi temperature is $T_F = \frac{E_F}{k_B} \approx 1 \mu\text{K}$. To increase the effective attraction, one may consider adding a shallow optical lattice. For instance with lattice strength $V = 6E_R$, the BCS transition temperature can reach around 3nK . A similar estimate can be obtained for ^{161}Dy atom which has a larger magnetic dipole moment of $10\mu_B$, the corresponding dipolar interaction strength is around two times larger than that of ^{167}Er . Under the same condition, the BCS transition temperature can reach around 50nK . Furthermore, taking advantage of recent experimental realization of Feshbach resonance in magnetic lanthanide atoms such as Er [45], the dipole-dipole interaction is highly tunable. The transition temperature is estimated to reach around $0.2 \mu\text{K}$ or even higher. This high transition temperature T_c makes it promising to obtain the Weyl superfluid state in experiments.

Conclusion. We propose that an anisotropic Weyl superfluid state can be realized in a 3D spinless dipolar Fermi gas. The crucial ingredient of our model is the direction-dependent effective attraction between dipoles generated by a rotating external field. The long-sought low-temperature analog of Weyl fermions of particle physics has been found in the quasi-particle excitations in this superfluid state. The stability and the transition temperature are also studied, which will be use-

ful for exploring this Weyl superfluid state in future experiments.

Acknowledgements. This work is supported by AFOSR (FA9550-12-1-0079), ARO (W911NF-11-1-0230), DARPA OLE Program through ARO, the Charles E. Kaufman Foundation and The Pittsburgh Foundation (B.L. and W.V.L.). X.L. acknowledges support by JQI-NSF-PFC and ARO-Atomtronics-MURI. L.Y. is supported by NSFC under Grant No. (11274022).

* Electronic address: liubophy@gmail.com

† Electronic address: w.vincent.liu@gmail.com

- [1] G. E. Volovik, *The Universe in a Helium Droplet* (Oxford University Press, 2003).
- [2] L. Balents, *Physics* **4**, 36 (2011).
- [3] X. Wan, A. M. Turner, A. Vishwanath, and S. Y. Savrasov, *Phys. Rev. B* **83**, 205101 (2011).
- [4] S. A. Yang, H. Pan, and F. Zhang, *Phys. Rev. Lett.* **113**, 046401 (2014).
- [5] K.-Y. Yang, Y.-M. Lu, and Y. Ran, *Phys. Rev. B* **84**, 075129 (2011).
- [6] G. Xu, H. Weng, Z. Wang, X. Dai, and Z. Fang, *Phys. Rev. Lett.* **107**, 186806 (2011).
- [7] A. A. Burkov and L. Balents, *Phys. Rev. Lett.* **107**, 127205 (2011).
- [8] P. Hosur, S. A. Parameswaran, and A. Vishwanath, *Phys. Rev. Lett.* **108**, 046602 (2012).
- [9] O. Vafek and A. Vishwanath, *Annual Review of Condensed Matter Physics* **5**, 83 (2014).
- [10] G. B. Halász and L. Balents, *Phys. Rev. B* **85**, 035103 (2012).
- [11] A. A. Zyuzin, S. Wu, and A. A. Burkov, *Phys. Rev. B* **85**, 165110 (2012).
- [12] T. Meng and L. Balents, *Phys. Rev. B* **86**, 054504 (2012).
- [13] T. Timusk, J. P. Carbotte, C. C. Homes, D. N. Basov, and S. G. Sharapov, *Phys. Rev. B* **87**, 235121 (2013).
- [14] M. Gong, S. Tewari, and C. Zhang, *Phys. Rev. Lett.* **107**, 195303 (2011).
- [15] Y. Xu, R.-L. Chu, and C. Zhang, *Phys. Rev. Lett.* **112**, 136402 (2014).
- [16] V. Galitski and I. B. Spielman, *Nature* **494**, 49 (2013).
- [17] K. Aikawa, A. Frisch, M. Mark, S. Baier, R. Grimm, and F. Ferlaino, *Phys. Rev. Lett.* **112**, 010404 (2014).
- [18] K. Aikawa, S. Baier, A. Frisch, M. Mark, C. Ravensbergen, and F. Ferlaino, *Science* **345**, 1484 (2014).
- [19] M. Lu, N. Q. Burdick, and B. L. Lev, *Phys. Rev. Lett.* **108**, 215301 (2012).
- [20] K. Baumann, N. Q. Burdick, M. Lu, and B. L. Lev, *Phys. Rev. A* **89**, 020701 (2014).
- [21] K.-K. Ni, S. Ospelkaus, M. H. G. de Miranda, A. Pe'er, B. Neyenhuis, J. J. Zirbel, S. Kotochigova, P. S. Julienne, D. S. Jin, and J. Ye, *Science* **322**, 231 (2008).
- [22] C.-H. Wu, J. W. Park, P. Ahmadi, S. Will, and M. W. Zwierlein, *Phys. Rev. Lett.* **109**, 085301 (2012).
- [23] M. A. Baranov, M. Dalmonte, G. Pupillo, and P. Zoller, *Chemical Reviews* **112**, 5012 (2012).
- [24] Y. Li and C. Wu, *Sci. Rep.* **2**, 392 (2012).
- [25] C. Wu and J. E. Hirsch, *Phys. Rev. B* **81**, 020508 (2010).
- [26] R. Qi, Z.-Y. Shi, and H. Zhai, *Phys. Rev. Lett.* **110**, 045302 (2013).
- [27] T. Shi, S.-H. Zou, H. Hu, C.-P. Sun, and S. Yi, *Phys. Rev. Lett.* **110**, 045301 (2013).
- [28] L. You and M. Marinescu, *Phys. Rev. A* **60**, 2324 (1999).
- [29] T.-S. Zeng and L. Yin, *Phys. Rev. B* **89**, 174511 (2014).
- [30] G. M. Bruun and E. Taylor, *Phys. Rev. Lett.* **101**, 245301 (2008).
- [31] B. Liu and L. Yin, *Phys. Rev. A* **86**, 031603 (2012).
- [32] N. R. Cooper and G. V. Shlyapnikov, *Phys. Rev. Lett.* **103**, 155302 (2009).
- [33] S. Giovanazzi, A. Görlitz, and T. Pfau, *Phys. Rev. Lett.* **89**, 130401 (2002).
- [34] S. Giorgini, L. P. Pitaevskii, and S. Stringari, *Rev. Mod. Phys.* **80**, 1215 (2008).
- [35] M. A. Baranov, M. S. Mar'enko, V. S. Rychkov, and G. V. Shlyapnikov, *Phys. Rev. A* **66**, 013606 (2002).
- [36] C.-K. Chan, C. Wu, W.-C. Lee, and S. Das Sarma, *Phys. Rev. A* **81**, 023602 (2010).
- [37] P. W. Anderson and P. Morel, *Phys. Rev.* **123**, 1911 (1961).
- [38] H. Weyl, *Zeitschrift Für Physik* **56**, 330 (1929).
- [39] R. Wei and E. J. Mueller, *Phys. Rev. A* **86**, 063604 (2012).
- [40] Y. Morita, M. Kohmoto, and K. Maki, *Phys. Rev. Lett.* **78**, 4841 (1997).
- [41] L. Jiang, L. O. Baksmaty, H. Hu, Y. Chen, and H. Pu, *Phys. Rev. A* **83**, 061604 (2011).
- [42] C. A. Regal and D. S. Jin, *Phys. Rev. Lett.* **90**, 230404 (2003).
- [43] S. Gupta, Z. Hadzibabic, M. W. Zwierlein, C. A. Stan, K. Dieckmann, C. H. Schunck, E. G. M. van Kempen, B. J. Verhaar, and W. Ketterle, *Science* **300**, 1723 (2003).
- [44] V. Gurarie and L. Radzihovsky, *Annals of Physics* **322**, 2 (2007).
- [45] A. Frisch, M. Mark, K. Aikawa, F. Ferlaino, J. L. Bohn, C. Makrides, A. Petrov, and S. Kotochigova, *Nature* **507**, 475 (2014).

Supplementary Materials

PATH INTEGRAL APPROACH

By introducing Grassmann fields $\phi(\mathbf{r}, \tau)$ and $\phi^*(\mathbf{r}, \tau)$, which represent fermion fields, the grand partition function of the system is expressed as (the units are chosen as $\hbar = k_B = 1$)

$$Z = \int D\phi D\phi^* e^{-S}, \quad (S1)$$

with the action

$$S[\phi, \phi^*] = S_0[\phi, \phi^*] + S_{int}[\phi, \phi^*],$$

and

$$S_0[\phi, \phi^*] = \int d\tau \int d^3\mathbf{r} \int d^3\mathbf{r}' \phi^*(\mathbf{r}, \tau) \left[\frac{\partial}{\partial \tau} - \frac{\nabla^2}{2m} - \mu \right] \delta(\mathbf{r} - \mathbf{r}') \phi(\mathbf{r}', \tau),$$

$$S_{int}[\phi, \phi^*] = \frac{1}{2} \int d\tau \int d^3\mathbf{r} \int d^3\mathbf{r}' \phi^*(\mathbf{r}, \tau) \phi^*(\mathbf{r}', \tau) V(\mathbf{r} - \mathbf{r}') \phi(\mathbf{r}', \tau) \phi(\mathbf{r}, \tau).$$

The quartic fermionic interaction term in the action in Eq. (S1) can be decoupled by introducing Hubbard-Stratonovich fields $\kappa(\mathbf{r}, \tau)$, $\lambda(\mathbf{r}, \mathbf{r}', \tau)$, and $\tilde{\Delta}(\mathbf{r}, \mathbf{r}', \tau)$. This leads to a partition function with the action

$$\begin{aligned} S[\phi, \phi^*, \kappa, \lambda, \lambda^*, \tilde{\Delta}, \tilde{\Delta}^*] = & - \int d\tau \int d^3\mathbf{r} \int d^3\mathbf{r}' \left\{ \frac{1}{2} [\kappa(\mathbf{r}, \tau) \right. \\ & \left. V^{-1}(\mathbf{r} - \mathbf{r}') \kappa(\mathbf{r}', \tau) + \frac{|\lambda(\mathbf{r}, \mathbf{r}', \tau)|^2}{V(\mathbf{r} - \mathbf{r}')} + \frac{|\tilde{\Delta}(\mathbf{r}, \mathbf{r}', \tau)|^2}{V(\mathbf{r} - \mathbf{r}')} \right\} \\ & - \int d\tau \int d^3\mathbf{r} \int d^3\mathbf{r}' [\phi^*(\mathbf{r}, \tau), \phi(\mathbf{r}, \tau)] \mathbf{G}^{-1} \begin{bmatrix} \phi(\mathbf{r}', \tau) \\ \phi^*(\mathbf{r}', \tau) \end{bmatrix}, \end{aligned}$$

where

$$\mathbf{G}^{-1}(\mathbf{r}, \mathbf{r}', \tau) = \frac{1}{2} \left(\mathbf{G}_0^{-1}(\mathbf{r}, \mathbf{r}', \tau) - \begin{bmatrix} 0 & \tilde{\Delta}(\mathbf{r}, \mathbf{r}', \tau) \\ -\tilde{\Delta}^*(\mathbf{r}, \mathbf{r}', \tau) & 0 \end{bmatrix} \right),$$

with

$$\mathbf{G}_0^{-1}(\mathbf{r}, \mathbf{r}', \tau) = \begin{bmatrix} G_0^{-1}(\mathbf{r}, \mathbf{r}', \tau) & 0 \\ 0 & -G_0^{-1}(\mathbf{r}', \mathbf{r}, \tau) \end{bmatrix},$$

and

$$G_0^{-1}(\mathbf{r}, \mathbf{r}', \tau) = - \left[\left(\frac{\partial}{\partial \tau} - \frac{\nabla^2}{2m} - \mu + \kappa(\mathbf{r}, \tau) \right) \delta(\mathbf{r} - \mathbf{r}') + \lambda(\mathbf{r}', \mathbf{r}, \tau) \right].$$

After integrating out the fermion fields, the effective action is obtained

$$\begin{aligned} S_{eff}[\kappa, \lambda, \lambda^*, \tilde{\Delta}, \tilde{\Delta}^*] = & - \int d\tau \int d^3\mathbf{r} \int d^3\mathbf{r}' \frac{1}{2} [\kappa(\mathbf{r}, \tau) \\ & V^{-1}(\mathbf{r} - \mathbf{r}') \kappa(\mathbf{r}', \tau) + \frac{|\lambda(\mathbf{r}, \mathbf{r}', \tau)|^2}{V(\mathbf{r} - \mathbf{r}')} + \frac{|\tilde{\Delta}(\mathbf{r}, \mathbf{r}', \tau)|^2}{V(\mathbf{r} - \mathbf{r}')} \\ & - Tr[\ln(-\mathbf{G}^{-1})]. \end{aligned}$$

Using the saddle point condition, the Hartree-Fock self-energy and superconducting gap are obtained as shown in Eq. (1).